

## *Chapter 7*

# **The effects of shallow rheological boundaries in the upper mantle on inducing shorter time scales of diapiric flows †**

P.E. van Keken, D.A. Yuen and A.P. van den Berg

### **Abstract**

We have studied the effects of rheological boundaries in the upper mantle on the dynamics of inducing pulsating diapiric plumes. We have compared the effects due to shallower rheological interfaces in the upper mantle on the time scales of the pulsations. Comparing with a basic model with a rheological interface at 670 km depth, we find that time scales between pulsations can be reduced considerably down to a few million years by adding another rheological boundary at 400 km depth. These results suggest that short time scale diapiric flows may be generated from relatively stationary upwellings from the lower mantle because of the presence of rheological boundaries in the shallow upper mantle.

---

† This chapter has been submitted to Geophysical Research Letters

## 7.1 Introduction

Phase boundaries have been recognized for a long time as being important for mantle dynamics [Vening Meinesz, 1962; Verhoogen, 1965; Christensen & Yuen, 1984]. It is only recently that rheological boundaries separating creep regimes have been identified in the laboratory [Karato, 1988; Karato & Li, 1992; Karato, 1992]. Its ramifications on mantle flows can be tremendous, as seen from the recent results by Van Keken et al. [1992], who studied the interaction between a mantle plume and the 670 km discontinuity as a rheological boundary. Diapiric instabilities with short time scales, as compared with over-turn time, were found to develop from this rheological boundary. In this work we will show how shallower transitions can introduce shorter pulsations. As rheological boundaries can be shallower than phase boundaries, they may serve as a shallow site for producing diapiric flows with very short time scales.

## 7.2 Model description

We model the mantle as an incompressible viscous fluid medium at infinite Prandtl number in the Boussinesq approximation. A non-Newtonian upper mantle lies over a Newtonian lower mantle. The dimensionless depth-varying creep law used in the computations is given by

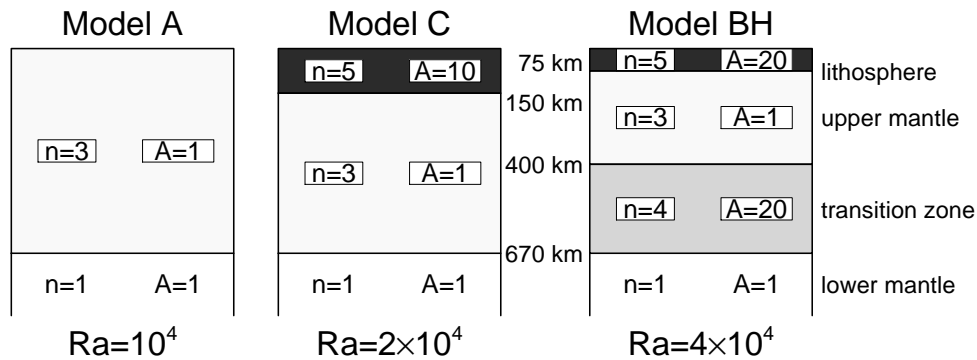


**Figure 7.1** Specification of the rheology parameters  $A(z)$  and  $n(z)$ , and the thermal Rayleigh number  $Ra$ , based on the lower mantle viscosity, for the three models.

$$\sigma_{ij} = A(z) \dot{\epsilon}^{1/n(z)-1} \dot{\epsilon}_{ij} \quad (7.1)$$

where  $\sigma_{ij}$  and  $\dot{\epsilon}_{ij}$  are the elements of respectively the deviatoric stress and strain-rate tensor,  $n(z)$  represents the depth variation of the power law index  $n$  in the mantle creep law,  $A(z)$  is the pre-exponential factor which varies with depth, and  $\dot{\epsilon}$  is the second invariant of the strain rate tensor. The non-dimensional differential equations describing conservation of mass, momentum and thermal energy are solved using a primitive variable finite element method, described in [Van den Berg et al., 1991; Van Keken et al., 1992]. The important control variables are  $n(z)$ ,  $A(z)$ , and the thermal Rayleigh number  $Ra$ . Calculations are performed in a rectangular box with aspect ratio of 3.5.

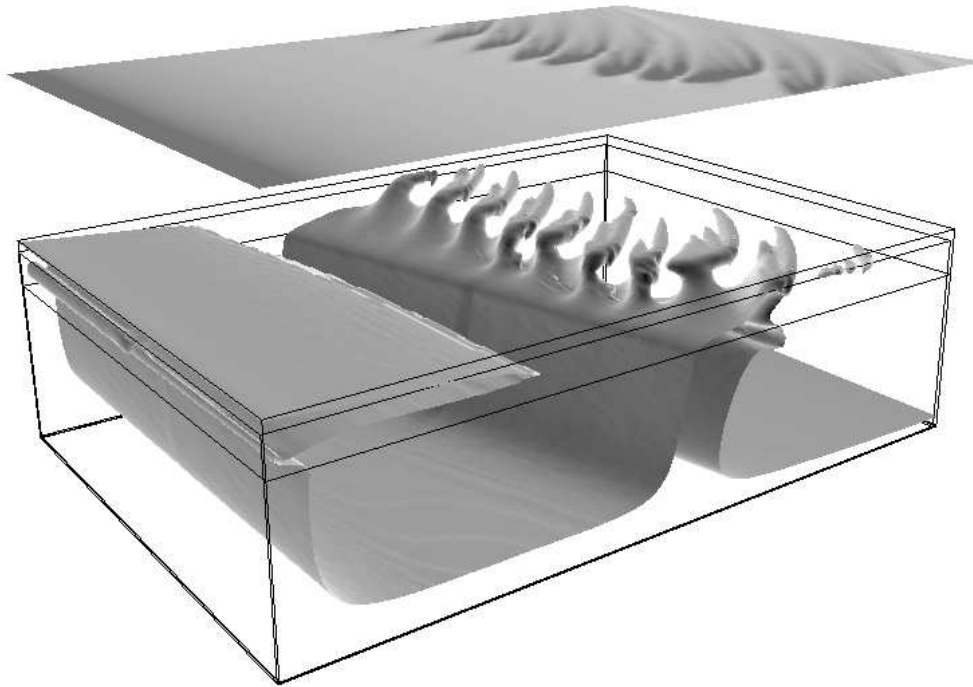


**Figure 7.2a** Temporal development of the three-layer model C. Time progresses along the third axis, away from the viewer. In the lower frame the isosurface of temperature  $T = 0.35$  is shown. Distinct diapiric structures are formed at the interface from the stationary plume in the lower mantle. The diapiric pulses correlate well with the peaks in the surface heat flow, shown in the top frame.

The three models considered in this work are depicted in figure 7.1. Model A and C are the non-Newtonian models used in [Van Keken et al., 1992]. In the third model, BH, we have included a representation of the 'hard garnet' rheology that has been proposed for the transition zone between 400 and 670 km depth [Karato, 1989; Meade & Jeanloz, 1990]. Increasing  $A(z)$  makes the rheology intrinsically harder. The thermal Rayleigh number (shown in figure 7.1) is based on the lower mantle Newtonian viscosity [Van den Berg et al., 1991], and increases from  $Ra = 10^4$  for model A to  $Ra = 4 \times 10^4$  for model BH.

### 7.3 Results

Snapshots displaying the development of temperature and stream function have already been displayed in [Van Keken et al., 1992] for models A and C. More detailed dynamics can be observed in a video available from the authors. Figure 7.2a shows the development of model C in a different way. The temporal evolution of the 2-D model is now depicted in a 3-D figure, in which time evolves in the third direction, pointing away from the viewer. The isosurface of  $T = 0.35$  is shown. The interior of the plume is relatively cold. This cold origin is due to the cold tongue produced by the plate-like character of the upper boundary layer [Van den Berg et al., 1991; Lenardic & Kaula, 1993], that enables the long extension of the cold mass at the bottom. Features present in the data by Van Keken et al. [1992], can be identified in figure 7.2a. From the stationary upwelling at the left hand side a long flat patch can be seen, showing the strong pulling motion of the large scale circulation due to the presence of the mobile lithosphere. From the upwelling lower mantle plume in the center, discrete thermal anomalies are shedded off the interface and drawn away from the plume by the large scale circulation. The diapirs consist of detached blobs and do not form a continuous conduit.

If the parameters are dimensionalized using a model mantle depth of 1800 km (accounting for the spherical to cartesian transformation) the pulsating behaviour of the plume in model C is shown for 300 Myr; the period between the pulsations is approximately 35 Myr. The viscosity in the upper mantle is on average 200 times lower than the viscosity in the lower mantle for both model A and C. In model C, the viscosity in the lithosphere changes drastically from stagnation zones, where the viscosity is around 1000, to the positions at the boundaries and above the mantle plume, where the strong shearing motion decreases the viscosity drastically in this strongly non-Newtonian ( $n = 5$ ) medium. The average viscosity of the lithosphere is around 1, corresponding to a dimensional viscosity of  $10^{22}$  Pa · s.

Figure 7.2b gives a similar view of the evolution of model BH, which is shown for dimensional time of 75 Ma. The isosurface for  $T = 0.42$  is shown. The

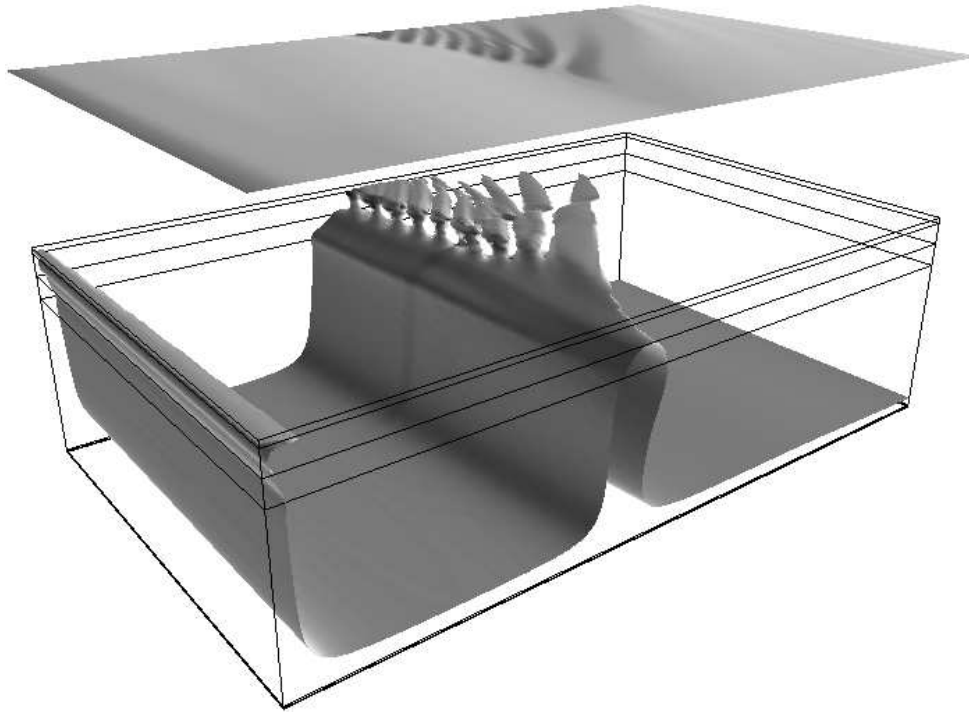


**Figure 7.2b** A similar view as in figure 7.2a, but now of the four-layer model BH. The isosurface is for  $T = 0.42$ . Very sharp diapiric structures are now formed at the 400 km discontinuity. Period between the pulsations is approx. 4 Myr.

average viscosity in each layer is 5 in the lithosphere,  $1/300$  in the upper mantle, and  $1/4$  in the transition zone. Above the first discontinuity at 670 km, the hot material contained in the plume can travel faster than in the underlying lower mantle. In model C this leads to periodic instabilities off the boundary layer that is formed on top of the plume at the 670 km discontinuity. In this model BH, the viscosity contrast across 670 is much smaller ( $1/4$  as compared to  $1/200$ ) and the faster transport leads only to a thinning of the plume in the transition zone, which remains stationary in time. At the top of the transition zone, at 400 km depth, the viscosity contrast is approximately  $1/80$ . Here the much faster transport of the hot material, helped by the non-Newtonian effects, leads again to the periodic pulsating flow. The discrete diapirs originating off the 400 km discontinuity are clearly visible in figure 7.2b. The 'hot tongue' emanating from the stationary upwelling at the left hand side boundary, prominently present in figure 7.2a, is strongly reduced in model BH (figure 7.2b). This is a consequence of the higher temperature indicated

by the isosurface, and the less dynamic large scale flow, caused by the thinner lithosphere (75 km as compared to 150 km), and the higher viscosity in the transition zone.

In Figure 7.3 we show a comparison of the dimensional surface heat flow as observed in the models A, C and BH. A common feature in the three models is the periodicity of the diapiric upwellings and the relative stationarity of the plume in the lower mantle. The periodicity decreases, from around 80 Myr for model A and 35 Myr for model C, to approximately 4 Myr for model BH. This increase of frequency is a consequence of the higher Rayleigh number (figure 7.1) and the shallower origin of the diapirs.

Figure 7.4 shows the maximum vertical velocity as observed in the direct vicinity of the upwelling plume. The dramatic decrease in the period between the diapirs between models C and BH is clearly visible. The maximum vertical velocity increases strongly from 3 cm/yr for model A and 4 cm/yr for model C to more than 15 cm/yr for model BH, again demonstrating the dynamical effect induced by the shallower level of the rheological interface. The velocities are much higher in

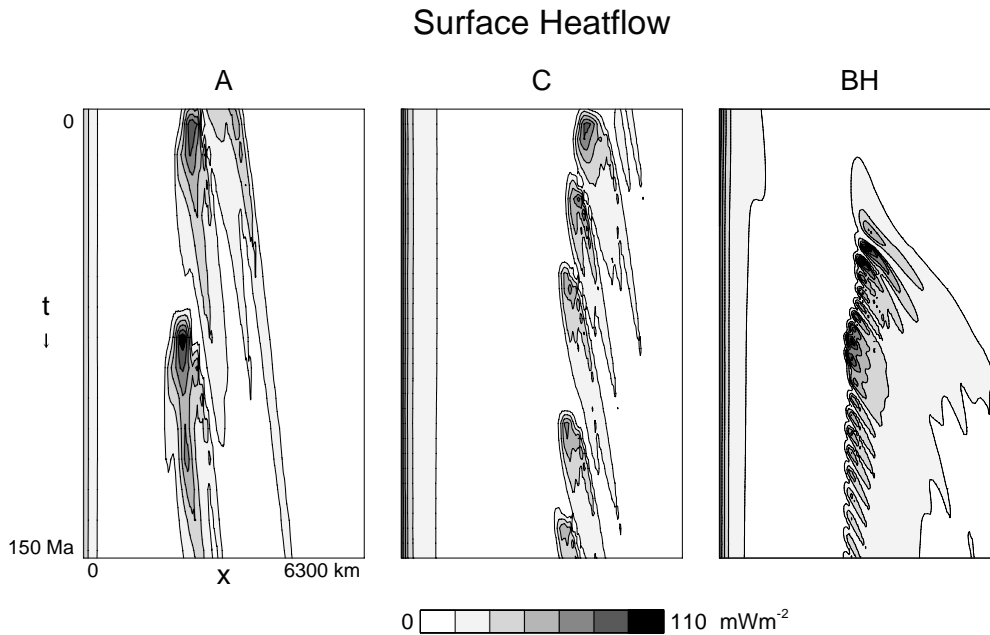


**Figure 7.3** Comparison of dimensional surface heatflow for the three cases.

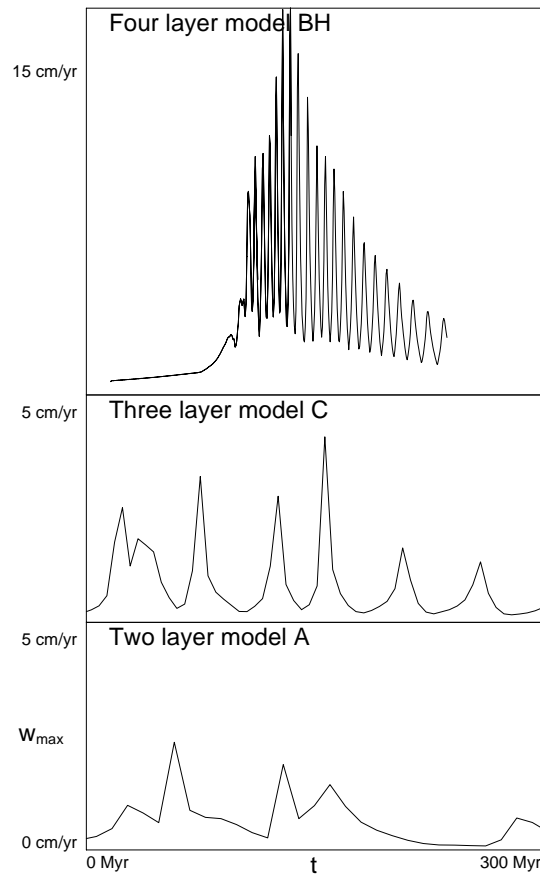


**Figure 7.4** Comparison of maximum dimensional upward velocity around the plume. The pulsating flow is much more frequent and faster for the four-layer model BH, than for the models A and C.

case BH compared with case A, but less volume is carried, resulting in approximately equal heat flow maxima above the diapirs for the two cases (figure 7.3). Heat flow maxima for models BH and A are around  $110 \text{ mW} \cdot \text{m}^2$ , close to an order of magnitude greater than the mean heat flow.

## 7.4 Discussion

In this work we have demonstrated the importance of rheological boundaries in upper mantle dynamics. An important feature of the dynamical models is the pulsating diapiric fbw, that produces discrete upwellings of hot material at a steady position under a moving lithospheric plate. This kind of behaviour is observed in hot spot volcanism of the type exemplified by the Hawaiian [Schilling, 1985] and Galapagos islands [Christie et al., 1992]. Thermodynamic phase transitions can also cause diapiric fbw, but their behaviour is not as regular [Liu et al., 1991; Zhao et al., 1992]. These type of models demonstrate that depth varying creep laws can explain, at least to some extent, the coexistence of a large scale fbw, as observed by the plate motions, and persistent small scale 'hot spots', as observed underneath mid-oceanic island chains. Both are expressions of the advective cooling of the Earth and seem to behave independently of each other at the time scales, less than 200 Myr, considered.

The pulsating behaviour of mantle upwellings is a consequence of the viscosity decrease over a rheological boundary, and in itself independent of the type of large scale fbw, whether it is whole, layered or intermittent mantle convection. Furthermore, one can expect that at shallow levels, less than 400 km, rheological transitions occur that are not connected with the major thermodynamical phase transitions between 400 and 670 km depth [e.g., Karato, 1992]. The shallower level of a rheological boundary can be envisaged to induce diapiric instabilities with time scales shorter than those found in present models. This mechanism might well be used to explain the temporal variations in magmatic activity as observed e.g. underneath island chains [Schilling, 1985; Christie et al. 1992], asthenospheric upwellings in rift zones [Tatsumi & Kimura, 1991], and at mid-oceanic ridges [Batiza et al., 1992; Gente et al., 1992].

## Acknowledgements

Support of this research has come from the Dutch NWO, the U.S. Army High Performance Computing Research Center, and the Geochemistry program of N.S.F., D.O.E., and N.A.T.O. We appreciate stimulating conversation with Shun Karato.